

# Searches for Heavy Quark States at ATLAS

Hok-Chuen (Tom) Cheng (on behalf of the ATLAS Collaboration)

University of Michigan, Ann Arbor, USA

E-mail: hccheng@umich.edu

**Abstract.** This talk highlights the latest results of heavy quark searches from the ATLAS collaboration, mainly on resonance searches and vector-like quarks (VLQs) searches. Searches for  $t\bar{t}$  resonances using lepton-plus-jets events in proton-proton collisions at center-of-mass energy of 8 and 13 TeV are presented. Limits are set for BSM particles such as topcolor-assisted technicolor  $Z'_{TC}$ , Kaluza-Klein (K-K) gluons  $g_{KK}$  and K-K excitations of graviton  $G_{KK}$  in the Randall-Sundrum model of extra dimensions. VLQs arise naturally in many models such as Little Higgs and Composite Higgs and typically couple preferably to the third generation SM quarks and weak bosons. Limits are set for vector-like bottom (B) and top (T) quarks decay to lepton-plus-jets final states via  $Hb+X$  and  $Ht+X$  channels in two analyses using 8 and 13 TeV datasets from ATLAS.

## 1. Introduction

There are two main categories of heavy quark searches at ATLAS [1]. Firstly, there are model-agnostic searches in which we look for resonances such as  $X \rightarrow t\bar{t}, t\bar{b}$  or single  $t+E_T^{miss}$ . Secondly, there are vector-like quark (VLQ) searches in which we look for either a pair of VLQs or a single VLQ production. This talk intends to give an overview and describe several examples of these two categories of searches.

## 2. Resonance Searches

### 2.1. Overview of Resonance Searches at ATLAS

ATLAS has several searches for resonances with different final states. At  $\sqrt{s} = 8$  TeV, there is a  $t\bar{t}$  resonance search using the lepton-plus-jet final state [2], a  $t\bar{b}$  resonance search using the lepton-plus-jet final state [3] and a  $t\bar{b}$  resonance search using the  $qqbb$  final state [4]. At  $\sqrt{s} = 13$  TeV, there is a  $t\bar{t}$  resonance search using the lepton-plus-jet final state looking for  $Z'$  [5]. The following sections focus on the two  $t\bar{t}$  resonance searches using the lepton-plus-jet final state.

### 2.2. $t\bar{t}$ Resonance Searches: Motivations

Several benchmark models predict new resonances decaying into  $t\bar{t}$ . For example, the topcolor-assisted technicolor  $Z'$ , which is a spin-1 color singlet, decays into  $t\bar{t}$ . In the Kaluza-Klein Randall-Sundrum model, the K-K excitation of gluon  $g_{KK}$  decays to  $t\bar{t}$  and is a spin-1 color octet. Also, there is the excited graviton  $G_{KK}$  which is a spin-2 color singlet and decays to  $t\bar{t}$ . There are other color singlet scalar particles which also decay into  $t\bar{t}$ .

The general strategy here is to select  $t\bar{t}$  events, then reconstruct the  $t\bar{t}$  invariant mass  $m_{t\bar{t}}$  and look for an excess or deviation from the Standard Model (SM) predicted  $t\bar{t}$  background.

36 2.3.  $t\bar{t}$  Resonance Searches at  $\sqrt{s} = 8$  TeV

37 This analysis uses the  $20.3 \text{ fb}^{-1}$  of data collected at the ATLAS detector at a center-of-mass  
 38 energy of 8 TeV in 2012. The events are categorized into two types depending on the topology.

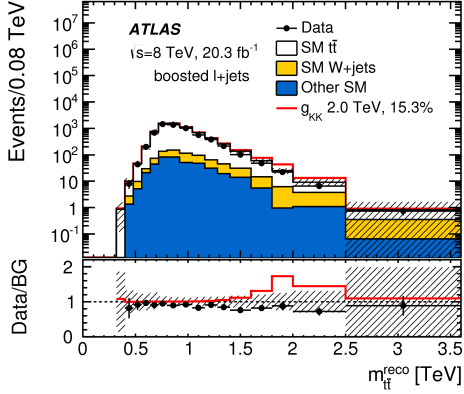


**Figure 1.** Reconstructed mass spectrum for the boosted topology overlaid with  $g_{KK}$  signal at 2.0 TeV. The ratio of data to SM background and signal is shown in the bottom. [2]

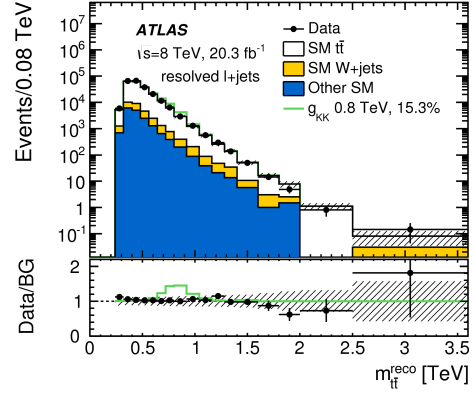


**Figure 2.** Reconstructed mass spectrum for the resolved topology overlaid with  $g_{KK}$  signal at 0.8 TeV. The ratio of data to SM background and signal is shown in the bottom. [2]

39 The first category is the boosted topology where the hadronic top is reconstructed using the  
 40 largest  $p_T$  large-R jet. At least one small-R jet must be b-tagged and matched to at least one of  
 41 the top candidates. The semi-leptonic top is reconstructed using  $E_T^{miss}$ , lepton, and the largest  
 42  $p_T$  small-R jet near jet. Events that failed to meet the requirement for the boosted topology will  
 43 pass to the selection for the resolved topology where at least 4 small-R jets are required and at  
 44 least one of them has to be b-tagged. In both categories, the b-tagged jet has to match to either  
 45 the hadronic-top jet, the leptonic-top jet or both, otherwise it is discarded. The reconstructed  
 46 mass  $m_{tt}^{reco}$  spectrum is scanned for deviations from the SM expectation as shown in figures 1 and  
 47 2. The search is performed on 6 boosted, 6 resolved and 6 combined channels and a deviation  
 48 is required in all channels at the same place.

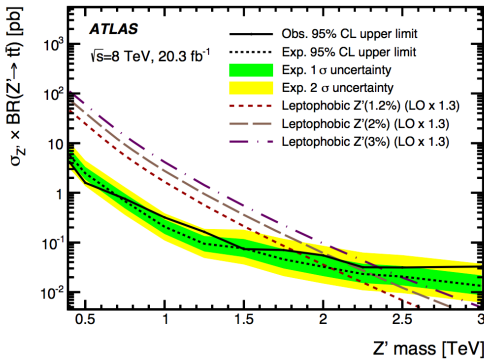


**Figure 3.** Limit plot for cross-section times branching fraction as a function of the  $Z'$  mass. [2]

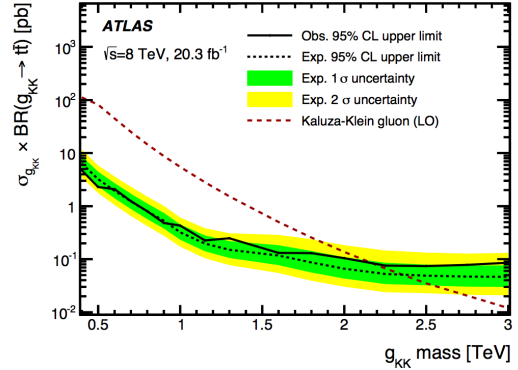


**Figure 4.** Limit plot for cross-section times branching fraction as a function of the  $g_{KK}$  mass. [2]

49 No excess above the SM prediction is observed. Cross-section limits are set for different  
 50 benchmark models. In particular, the topcolor-assisted technicolor  $Z'$  has been excluded between  
 51 0.4 TeV and 1.8 TeV at 95% confidence level (CL). The K-K gluon in the R-S model  $g_{KK}$  has  
 52 been excluded between 0.4 TeV and 2.2 TeV at 95% CL. The corresponding limit plots are shown  
 53 in figures 3 and 4. This analysis is not sensitive enough to set any limit to the K-K graviton or  
 54 the color singlet scalar particle.

#### 55 2.4. $t\bar{t}$ Resonance Searches at $\sqrt{s} = 13$ TeV

56 This analysis uses  $3.2 \text{ fb}^{-1}$  data collected at the ATLAS detector at  $\sqrt{s} = 13$  TeV in 2015. In  
 57 each event, exactly one lepton is reconstructed and must match candidates that triggered the  
 58 event. For the leptonic-top b-jet, at least one small-R jet is reconstructed in the  $\Delta R(l, \text{jet}) < 1.5$   
 59 cone. For the hadronic-top jet, at least one top-tagged large-R jet is reconstructed in the  $\Delta\phi(l,$   
 60 large-R jet)  $> 2.3$  and  $\Delta\phi(\text{leptonic-top jet, large-R jet}) > 1.5$  region. In addition, at least one  
 61 b-tagged small-R jet is reconstructed.

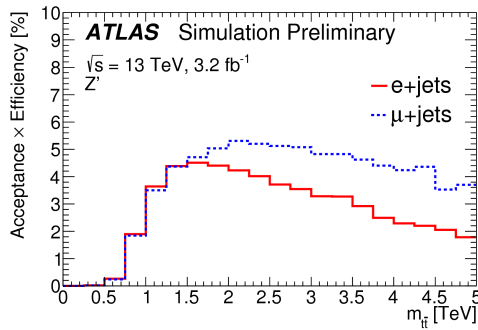


**Figure 5.** Acceptance times efficiency for the  $e$ +jets and  $\mu$ +jets channels as a function of the  $Z'$  mass. [5]

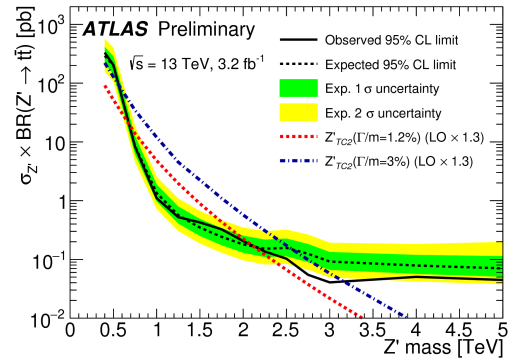


**Figure 6.** Limit plot for cross-section times branching fraction as a function of the reconstructed  $Z'$  mass. [5]

62 The acceptance times efficiency for  $e$ +jets and  $\mu$ +jets channels as a function of reconstructed  
 63 mass  $m_{t\bar{t}}$  is shown in figure 5. The  $e$ +jets channel has lower acceptance times efficiency for  $m_{t\bar{t}}$   
 64 above 1.5 TeV because of the inefficiency of  $e^-$  ID and overlap removal in highly boosted top  
 65 quarks. The major sources of systematic uncertainties are the large-R jet energy scale, the light  
 66 flavor and charm jet mistag rate and luminosity. No excess above the SM prediction is observed.  
 67 The topcolor-assisted technicolor  $Z'$  has been excluded from 0.7 TeV to 2.7 TeV at 95% CL and  
 68 the corresponding limit plot is shown in figure 6.

### 69 3. Vector-like Quark (VLQ) Searches

#### 70 3.1. VLQ Searches: Motivations

71 VLQs that arise naturally in models alternative to supersymmetry such as the Little Higgs [6, 7]  
 72 and the Composite Higgs [8, 9] have no Yukawa coupling to the newly discovered Higgs boson  
 73 and are therefore not constrained by the recent Higgs measurements. They typically couple  
 74 preferentially to the third generation quarks and can have flavor-changing neutral current decays.  
 75 They can be pair-produced via QCD below 1 TeV and can be dominated by single production at  
 76 high mass, depending on the weak couplings to the gauge bosons. Depending on the models, 4  
 77 types of VLQs exist. They include the vector-like T ( $Q = +2/3$ ), B ( $Q = -1/3$ ), X ( $Q = +5/3$ )  
 78 and Y ( $Q = -4/3$ ) quarks. The branching ratio of B and T quarks for different models are  
 79 shown in figures 7 and 8.

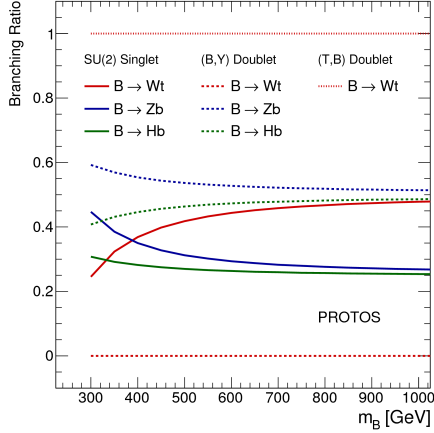


**Figure 7.** Branching ratio of  $SU(2)$  singlet,  $(B,Y)$  and  $(T,B)$  doublet models as a function of the B quark mass. [10]

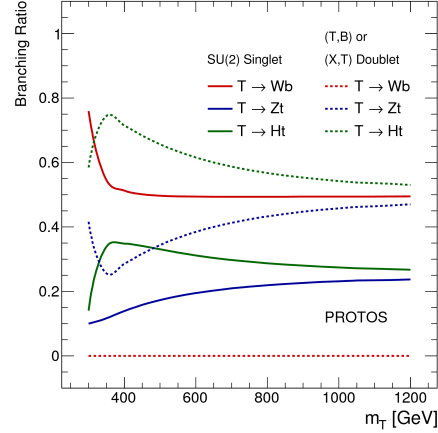


**Figure 8.** Branching ratio of  $SU(2)$  singlet,  $(T,B)$  and  $(X,T)$  doublet models as a function of the T quark mass. [10]

### 3.2. Vector-like Bottom ( $B$ ) and Top ( $T$ ) Quark Searches at ATLAS

There are several searches for VLQs at ATLAS, each sensitive to different decay modes. At  $\sqrt{s} = 8$  TeV, there is one for VLQs that decay into a  $Z$  boson and a third-generation quark [11] and another one for the final state of b-jets and a pair of leptons of the same charge [12]. In the following sections, searches for pair production of VLQ and of four top quarks in the lepton-plus-jets final state at 8 TeV [10] and 13 TeV [13] will be described.

### 3.3. $B$ Quark Search using $Hb \rightarrow X$ Decay Mode at 8 TeV

The sample dominated by  $t\bar{t}$  is selected and is sub-divided into 8 categories using jet multiplicity  $n_{jets}$ , b-multiplicity and the mass of the closest two jets. Background rich regions have low b-multiplicity and signal rich regions are dominated by high b-multiplicity events. The search is done in the distribution of the scalar sum of the transverse momentum of jets,  $l^\pm$  and  $E_T^{miss}$  ( $H_T$ ). The  $H_T$  distribution for the signal rich regions are shown in figure 9.

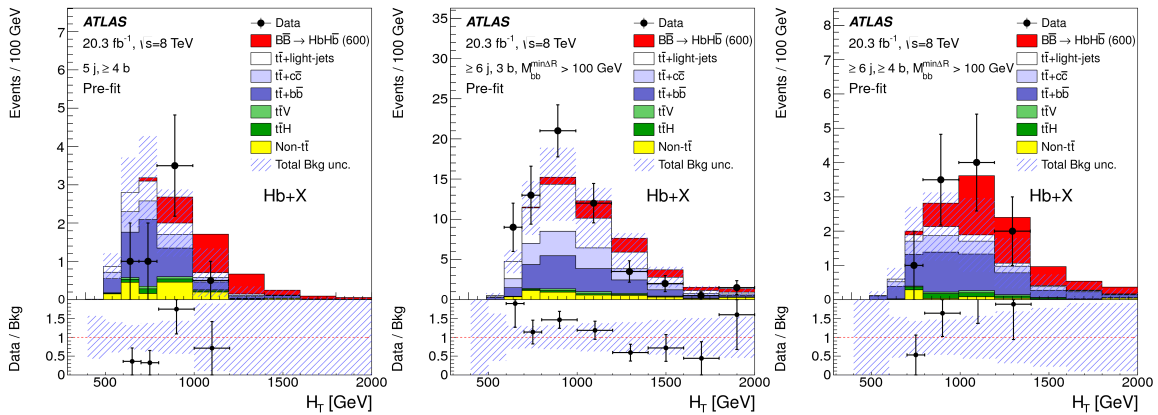


**Figure 9.**  $H_T$  distribution of the signal rich regions. [10]

The major systematic uncertainties are the jet energy scale and the theoretical cross-section. No excess above the SM prediction is observed. Assuming  $\mathcal{BR}(B \rightarrow Hb) = 1$ ,  $m_B$  is excluded

94 from 350 GeV to 580 GeV and from 635 GeV to 700 GeV at 95% CL with expected exclusion  
 95 region below 625 GeV. In the SU(2) singlet model,  $m_B$  is excluded below 735 GeV at 95% CL  
 96 with expected exclusion region below 635 GeV. The results are summarized in the exclusion  
 97 limit plots as shown in figure 10.

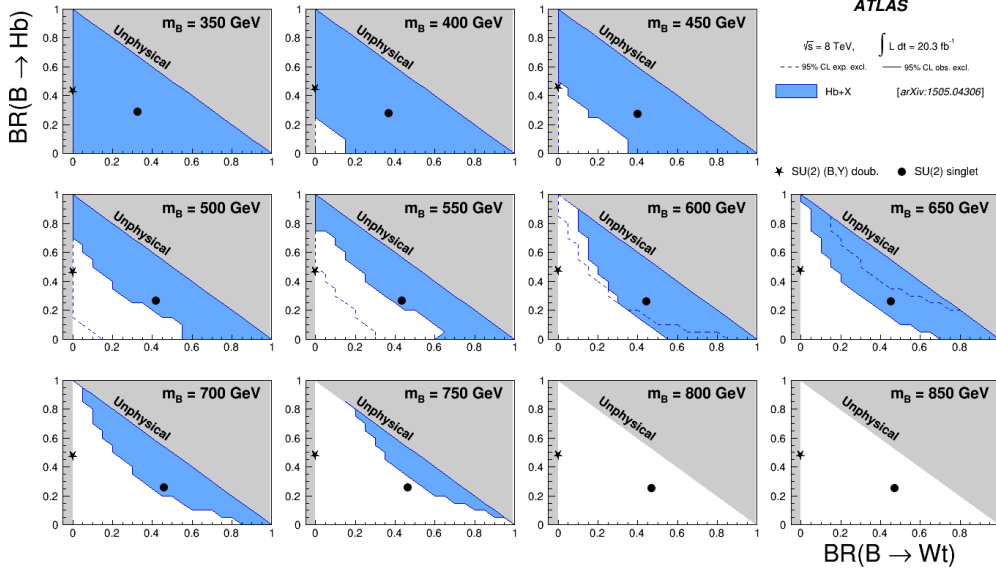


**Figure 10.** 2D exclusion limit plots of  $\mathcal{BR}(B \rightarrow Hb)$  vs  $\mathcal{BR}(B \rightarrow Wt)$  for the B quark mass  $m_B$  ranging from 350 GeV to 850 GeV. [10]

### 98 3.4. T Quark Search using $Ht \rightarrow X$ Decay Mode at 13 TeV

99 The sample is sub-divided into 20 categories using jet multiplicity  $n_{jets}$ , b-multiplicity, the  
 100 mass of the two closest jets and the number of large-R jets with mass greater than 100 GeV.  
 101 The background rich regions have low b-multiplicity while the signal rich regions have high  
 102 b-multiplicity. The search is done using the distribution of the scalar sum of the transverse  
 103 momentum of jets,  $l^\pm$  and  $E_T^{miss}$  ( $m_{eff}$ ) using a binned likelihood fit under the background-only  
 104 hypothesis. The  $m_{eff}$  distribution of the signal-sensitive regions are shown in figure 11.

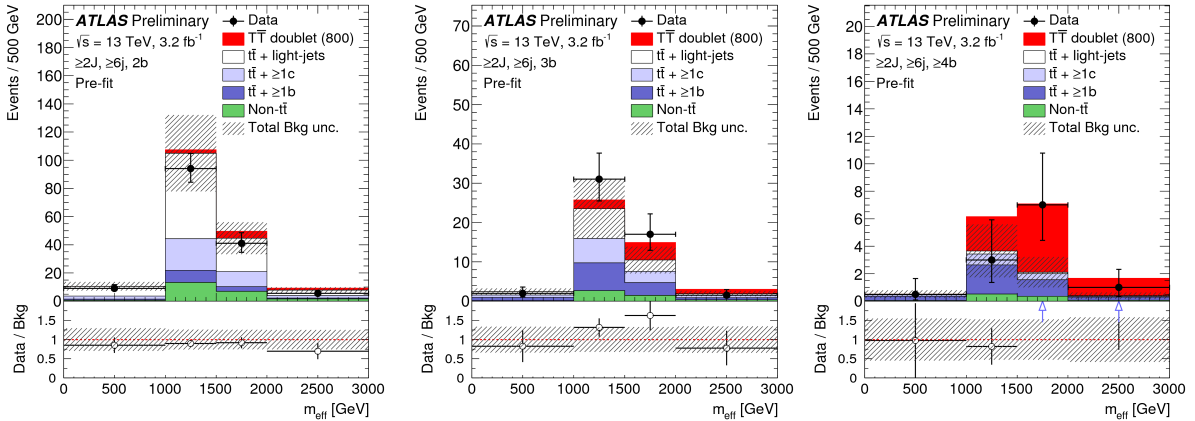


**Figure 11.**  $m_{eff}$  distribution of the signal-sensitive regions. [13]

105 The main systematic uncertainties include background production cross-section, which  
 106 includes factorization and renormalization scales and parton distribution function uncertainty  
 107 both at NLO and NNLO, luminosity and the jet energy scale. No excess above the SM prediction  
 108 is observed. Under the  $\mathcal{BR}(T \rightarrow Ht) = 1$  hypothesis,  $m_T$  is excluded below 900 GeV with an  
 109 expected exclusion region below 980 GeV at 95% CL. In the SU(2) singlet model,  $m_T$  is excluded  
 110 below 750 GeV with an expected exclusion region below 780 GeV at 95% CL. In the SU(2)  
 111 doublet model,  $m_T$  is excluded below 800 GeV with an expected exclusion region below 900 GeV  
 112 at 95% CL. The cross-section limits as a function of the T quark mass are shown in figure 12.  
 113 The 13 TeV analysis sensitivity reaches 950 GeV, exceeding that of 8 TeV analysis. However,  
 114 the observed limits are weaker than expected above 700 GeV due to statistical fluctuations in  
 115 data.

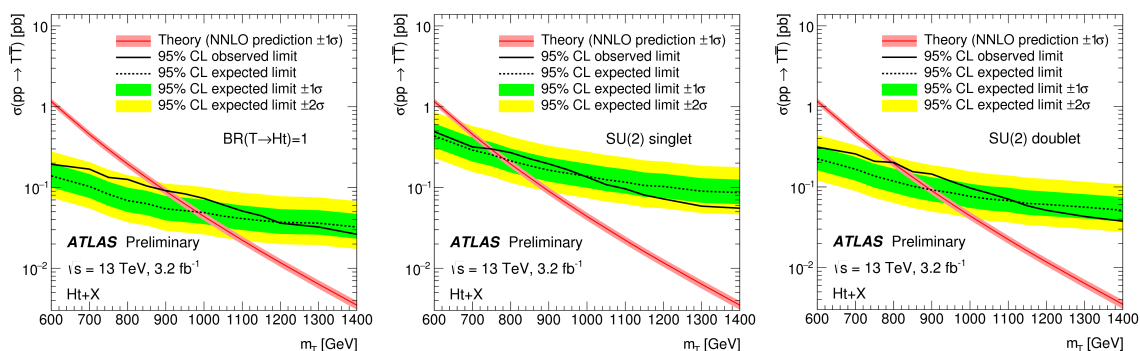


**Figure 12.** Cross-section limit plots as a function of the T quark mass  $m_T$  under  $\mathcal{BR}(T \rightarrow Ht) = 1$ , SU(2) singlet and SU(2) doublet hypotheses. [13]

#### 116 4. Acknowledgement

117 I am grateful to the ATLAS speakers committee for providing me the opportunity to give this  
 118 talk at the BEACH 2016 conference. I would also like to express my gratitude to the ATLAS  
 119 conveners Joseph Haley, Danilo Enoque Ferreira De Lima and Koji Terashi for their invaluable  
 120 advice and suggestions during the preparation of this talk.

#### 121 References

- 122 [1] ATLAS Collaboration 2008 *JINST* **3** S08003  
 123 [2] ATLAS Collaboration 2015 *Journal of High Energy Physics* **2015** 1–54 ISSN 1029-8479  
 124 [3] ATLAS Collaboration 2015 *Physics Letters B* **743** 235 – 255 ISSN 0370-2693  
 125 [4] ATLAS Collaboration 2015 *The European Physical Journal C* **75** 1–23 ISSN 1434-6052  
 126 [5] ATLAS Collaboration 2016 Search for heavy particles decaying to pairs of highly-boosted top quarks using  
 127 lepton-plus-jets events in proton–proton collisions at  $\sqrt{s} = 13$  TeV with the ATLAS detector Tech. Rep.  
 128 ATLAS-CONF-2016-014 CERN Geneva  
 129 [6] Arkani-Hamed N, Cohen A G, Katz E and Nelson A E 2002 *Journal of High Energy Physics* **2002** 034  
 130 [7] Schmaltz M and Tucker-Smith D 2005 *Annual Review of Nuclear and Particle Science* **55** 229–270 (Preprint  
 131 <http://dx.doi.org/10.1146/annurev.nucl.55.090704.151502>)  
 132 [8] Kaplan D B, Georgi H and Dimopoulos S 1984 *Physics Letters B* **136** 187 – 190 ISSN 0370-2693  
 133 [9] Agashe K, Contino R and Pomarol A 2005 *Nuclear Physics B* **719** 165 – 187 ISSN 0550-3213  
 134 [10] ATLAS Collaboration 2015 *Journal of High Energy Physics* **2015** 1–86 ISSN 1029-8479  
 135 [11] ATLAS Collaboration 2014 *Journal of High Energy Physics* **2014** 1–54 ISSN 1029-8479  
 136 [12] ATLAS Collaboration 2015 *Journal of High Energy Physics* **2015** 1–51 ISSN 1029-8479  
 137 [13] ATLAS Collaboration 2016 Search for production of vector-like top quark pairs and of four top quarks in  
 138 the lepton-plus-jets final state in  $pp$  collisions at  $\sqrt{s} = 13$  TeV with the ATLAS detector Tech. Rep.  
 139 ATLAS-CONF-2016-013 CERN Geneva